Excited state intramolecular proton transfer in 5-hydroxy flavone: A DFT study

ARTICLE *in* JOURNAL OF MOLECULAR STRUCTURE THEOCHEM · DECEMBER 2007

Impact Factor: 1.37 · DOI: 10.1016/j.theochem.2007.08.014

6 AUTHORS, INCLUDING:

Sudipta Dalai
Vidyasagar University
73 PUBLICATIONS **837** CITATIONS
SEE PROFILE

Ajay Misra
Vidyasagar University
56 PUBLICATIONS **910** CITATIONS
SEE PROFILE

ELSEVIER

Journal of Molecular Structure: THEOCHEM 824 (2007) 8–14

THEO CHEM

www.elsevier.com/locate/theochem

Excited state intramolecular proton transfer in 5-hydroxy flavone: A DFT study

Sankar Prasad De, Sankarlal Ash, Harekrishna Bar, Dipak Kumar Bhui, Sudipta Dalai, Ajay Misra *

Department of Chemistry and Chemical Technology, Vidyasagar University, Midnapore 721 102, West Bengal, India

Received 12 April 2007; received in revised form 13 August 2007; accepted 14 August 2007
Available online 29 August 2007

Abstract

Potential energy surfaces (PES) for the ground and excited state intramolecular proton transfer (ESIPT) processes in 5-hydroxy-flavone (5HF) were studied using DFT-B3LYP/6-31G(d) and TD-DFT/6-31G(d) level of theory, respectively. Our calculations suggest the non-viability of ground state intramolecular proton transfer (GSIPT) in 5HF. Excited states PES calculations support the existence of ESIPT process in 5HF. ESIPT in 5HF has been explained in terms of HOMO, LUMO electron density of the enol and keto tautomer of 5HF. PES scan by phenyl group rotation suggests that the twisted form, i.e., phenyl group rotated by 18.7° out of benzo-γ-pyrone ring plane is the most stable conformer of 5HF.

Keywords: Excited state intramolecular proton transfer; Intra molecular hydrogen bond; 5-Hydroxy flavone; DFT; Potential energy

1. Introduction

ESIPT is a reaction of tautomerization occurring in the excited states of molecules, in which proton is transferred via intramolecular H-bond or H-bonding bridge formed by solvent molecules [1,2]. The electronic excitation of the normal enol form (N) leads to the excited (N^*) form, which in the course of photochemical reaction is transformed into a proton transferred keto tautomer (T^*). 'T^*' relaxes radiatively or non-radiatively to the metastable ground state keto tautomer 'T', which converts to 'N' state via reverse proton transfer.

Flavonoids are a group of naturally occurring polyphenolic compounds ubiquitously found in fruits and vegetables [3–5]. The various classes of flavonoids differ in the level of oxidation of the '*C*' ring (Scheme 1) of the basic benzo-γ-pyrone structure. Common family members of flavonoids include flavones, flavanes, flavonols, catechins and anthocyanidins. Flavonols are flavonoids of particular importance because they have been found to possess antioxidant and free radical scavenging activity in foods [6]. More than 85% of these naturally occurring flavonols have a hydroxyl group in the 5 position and a sugar linkage in the 3 position [7]. Matsuura [7] demonstrated that the 5-hydroxyl moiety is responsible for the remarkable photochemical stability of flavonols and suggested that it provides an important biological function in protecting plants from photo degradation. Flavonols (3HF, 5HF) are presenting considerable interest not only in drug design [8], but also in the design of new fluorescence probes with broad applications in the study of molecular interactions in solutions and biological systems. The attractive features of flavonols are related to their high sensitivity to physicochemical parameters of the environment. Flavonols usually exhibit two bands in their fluorescence spectrum, due to ESIPT reaction, leading to two excited forms, the normal N^* and the tautomer T^* ones, and thus resulting in two strongly separated band in the fluorescence spectrum. Their positions and relative intensities depend on several parameters of the medium. Due to this unique phenome-

* Corresponding author. Tel.: +91 9433 220206; fax: +91 3222 275329.
E-mail address: ajaymsr@yahoo.co.in (A. Misra).

0166-1280/$ - see front matter © 2007 Elsevier B.V. All rights reserved.
doi:10.1016/j.theochem.2007.08.014

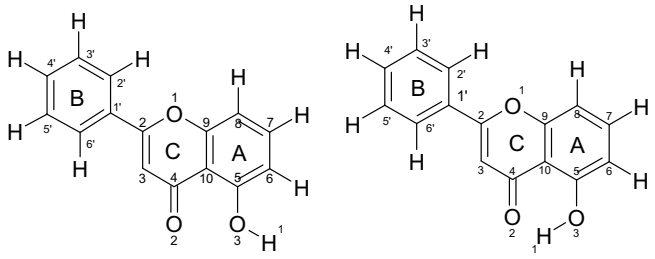

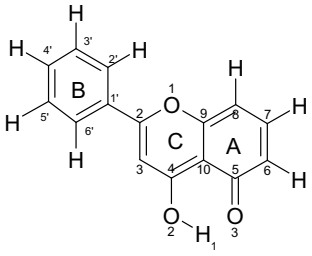

Scheme 1.

non many flavonol derivatives were shown to be very effective probes in the analysis of the structure of micelles [9–11] and phospholipid vesicles [12–14] as well as in the fluorescence recognition of cations of different radii [15,16] For these reasons, there is a considerable interest in the photophysics of 3- and 5- substituted flavones as model for complex natural flavonols.

5HF was once recognized as a completely 'nonluminescent' molecule. Recently, the resolution of fluorescence spectrum of 5HF has been achieved by using laser induced fluorescence technique. With the help of laser induced fluorescence study Chou et al. [17] showed dual emission band for 5HF maximized at 420 nm and 700 nm, respectively. The 420 nm band is normal emission band and the 700 nm band is assigned as the tautomeric emission band arises due to excited states intramolecular proton transfer in 5HF. It is now well established that both 3HF and 5HF show dual emission band. But unlike 3HF, it took quite a long time, till the invention of laser induced fluorescence technique, to establish the dual emission band of 5HF.

Since the original work of Weller [18] on the ESIPT of methyl salicylate (MS), a large number of experimental [19–26] and theoretical [27–33] studies on the ESIPT on a variety of systems have been reported. Among them, MS[34–40] and its related compounds, *O*-hydroxy-acetophenone (OHAP) [41–43] and *O*-hydroxy-benzaldehyde (OHBA) [44–47] have been well studied as prototypes of molecules showing ESIPT process. As far as the theoretical studies on proton transfer are concerned, there is no such unified methodology to understand the inner intricacies involved in this process. Hybrid HF/DFT methods have been proposed as a reliable tools for electronic computation in a general protocol for studying static and dynamic properties of hydrogen-bonded systems [48–50]. One such method, B3LYP [51] was evaluated by Barone et al. [52] and found that the results are in good agreement between DFT and MP2 results for structural and energy parameters. In view of its wide spread success for the calculation of large molecules [50], we decided to choose density functional approach for the present calculation of ESIPT process in 5HF.

2. Theoretical calculations

All calculations reported in this paper were carried out using the Gaussian 03 suite programs [53]. We compared the results for a number of methods and basis sets and found that DFT based calculations using hybrid functional (B3LYP) with 6-31G(d) basis set to be the optimal one in terms of price-performance ratio for carrying out elaborate electronic structure calculations within our limited computational resource. Analytic vibrational frequency computations at the optimized structure were done to confirm the optimized structure to be an energy minimum or a transition state structure.

Strength of the intramolecular hydrogen bond (IMHB) in the stable form of 5HF was evaluated as the difference between the (B3LYP/6-31G(d)) energy of the fully optimized structure of the non-hydrogen bonded form (Scheme 1, enol (open)) and the optimized energy of the 'N'-tautomer.

The evaluation of potential energy surface (PES) that describes the proton motion entails a molecular structure optimization. Ground state intramolecular proton transfer (GSIPT) curve was calculated by fixing the O–H distance over the range 0.80–2.00 Å and then rest of the geometry was optimized with DFT-B3LYP/6-31G(d) level of theory. Information on the ESIPT mechanism was obtained by calculating the Franck-Condon (FC) energies for the DFT (B3LYP)/6-31G(d) ground state structures at the TD-DFT (B3LYP)/6-31G(d) level. The FC curves for the proton transfer processes were obtained by adding the TD-DFT (B3LYP)/6-31G(d) excitation energies to the corresponding GSIPT curves.

3. Results and discussion

Before addressing the central problem, i.e., ESIPT in 5HF, we decided to optimize the method and basis that we like to use extensively for the potential energy calculations. Table-1a to 1c (see supplementary data) list the bond length, bond angle, dihedral angle obtained using HF/6-31G(d), DFT-B3LYP/6-31G, DFT-B3LYP/6-31G(d) level of theory, respectively, and also the same parameters obtained by M. Shoja [54] in their X-ray crystal structure study. In conformity with the experimental geometry, both the level of theory (HF and DFT) predicts that the enol tautomeric form is the stable structure in the ground state. Again the phenyl torsional angle obtained by DFT-B3LYP/6-31G under-estimate the experimental results

but the other two methods, i.e., HF/6-31G(d) and DFT-B3LYP/6-31G(d) overestimate the data as compare to its experimental value. On the other hand, DFT-B3LYP/6-31G(d) calculated geometry of the intramolecular hydrogen bonded ring, is in significantly better agreement with the experimental data than the other methods. Since for ESIPT processes, the chromophore of interest are involved in IMHB, we believe DFT-B3LYP/6-31G(d) level of theory will be more reliable methodology than the other two, for the present potential energy calculations.

Bond angle, dihedral angle data of Table-1b and 1c (see supplementary data) suggest that the six membered ring formed due to IMHB is planar and it is in the same plane that of benzo-γ-pyrone ring. Bond length data also suggest that the π-electron of IMHB ring involve in conjugation with the π-electron of benzo-γ-pyrone ring. The value of O(2)–H(1) bond distance (1.7 Å) in Table-1a (given as supplementary data) suggests that an intramolecular hydrogen bond is present between the H(1) of phenolic-OH group and O(2) of carbonyl group of the benzo-γ-pyrone ring.

Strength of the intramolecular hydrogen bond of the enol form ('N') is calculated by rotating the phenolic –OH group out of the hydrogen bonded conformation and computing the difference in energy between the closed and open form (Scheme 1) as shown in Fig. 1. Fig. 1 shows that the energy of 5HF is minimum when the torsional angle, H(1)–O(3)–C(5)–C(10) is 0° and energy increases with the increase in torsional angle, reaches a maximum (19.00 kcal/mol) at ~115° and then decreases to a value of ca. 14.95 kcal/mol until the torsional angle reaches to 180°. As the torsional angle is 0°, there is a strong IMHB present within the intramolecular six membered ring system involving hydroxyl group at 5 positions and the carbonyl group at 4 position of 5HF and at 180° (Scheme 1, 5HF enol(open)), the –OH group is free from any intramolecular hydrogen bonding interactions. Thus the difference in energy from the out of IMHB ring conformation to the IMHB ring conformation can be considered as a measure of IMHB strength. We found that the IMHB strength in 5HF is 14.95 kcal/mol, and the barrier for phenolic –OH rotation is nearly 19.00 kcal/mol.

Now, the conversion from 'N' to 'T' in the ground electronic state can be thought of as arising due to the transfer of proton from O(3) to O(2) with simultaneous redistribution of electron density within the six-membered hydrogen bonded ring. Some authors [55] have considered the O(3)–O(2) distance as fixed and varied the O(3)–H(1) bond distance to get an idea about the potential energy curve for both GSIPT and ESIPT processes.

A plot of O(2)–O(3) distance as a function of $r_{O(3)–H(1)}$, as shown in Fig. 2 revels that as the proton shifted from O(2) to O(3), the O(2)–O(3) distance changes significantly. At smaller O(3)–H(1) distance (0.70–0.90 Å), the O(2)–O(3) distance remain almost constant. But as the proton shifted further from O(3) it decreases sharply passes through a minimum and then enlarges to a distance comparable to that in 'T' form. It is specially interesting that, while the length of O(2)–O(3) bond is the same for the enol (at $r_{O(3)–H(1)} = 1$ Å) and keto form ($r_{O(3)–H(1)} = 1.6$ Å), the proton transfer results in considerable shortening of the O(2)–O(3) bond length, which is minimum at nearly halfway through the transfer (e.g., $r_{O(3)–H(1)} = 1.3$ Å see Fig. 2). Thus the closer approach of the oxygen atoms at the proton transfer midpoint ($r_{O(3)–H(1)} = 1.3$ Å) is favored energetically.

Fig. 3 shows the variation of O(3)–H(1)–O(2) angle as a function of $r_{O(3)–H(1)}$ distance. The O(3)–H(1)–O(2) angle increases with the increase of $r_{O(3)–H(1)}$ distance, reaches a maximum value at $r_{O(3)–H(1)} = 1.3$ Å and then decreases with further increase of $r_{O(3)–H(1)}$ distance. Similar to the O(2)–O(3) bond length variation with respect to $r_{O(3)–H(1)}$ Fig. 3 also shows that the O(3)–H(1)–O(2) bond angle is

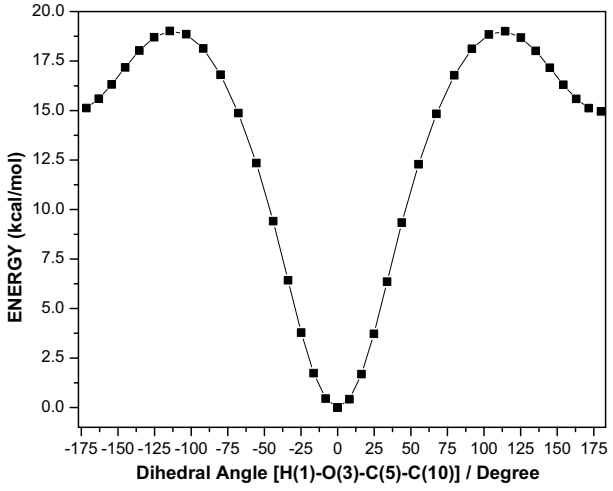

Fig. 1. Energetics of the transformation from IMHB from (N) to the non-hydrogen bonded form (hydroxyl group rotated from 0 to ±180°) of 5HF. For each value of dihedral angle [H(1)–O(3)–C(5)–C(10)], the geometry has been optimized using the DFT-B3LYP/6-31G(d) level of theory.

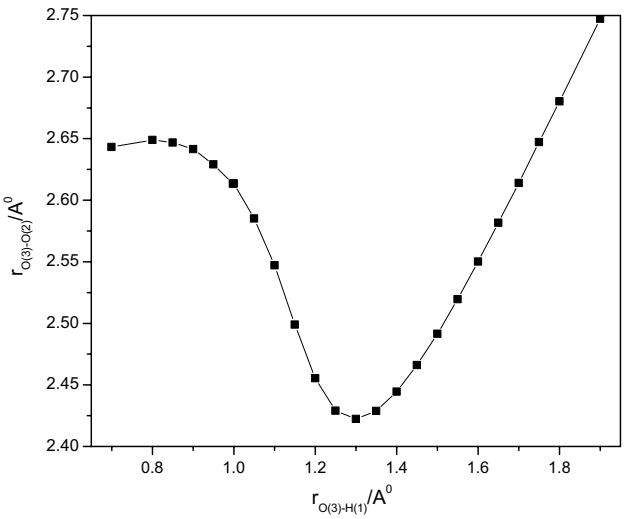

Fig. 2. Variation of O(3)–O(2) distance of 5HF with $r_{O(3)–H(1)}$ as obtained from DFT-B3LYP/6-31G(d) level of theory.

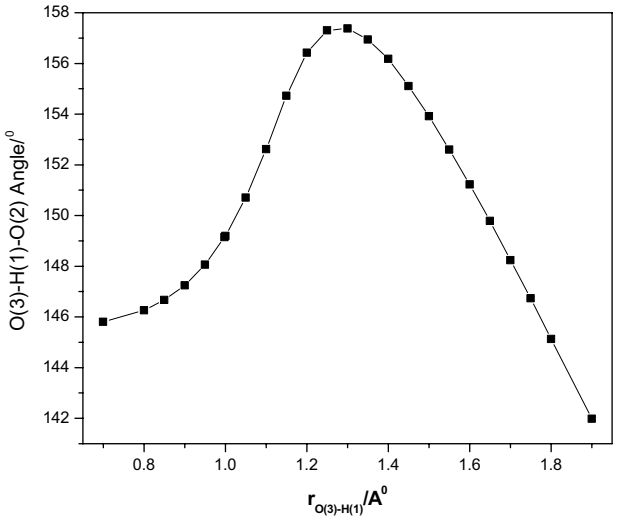

Fig. 3. Variation of O(3)–H(1)–O(2) angle of 5HF with $r_{O(3)-H(1)}$ as obtained from DFT-B3LYP/6-31G(d) level of theory.

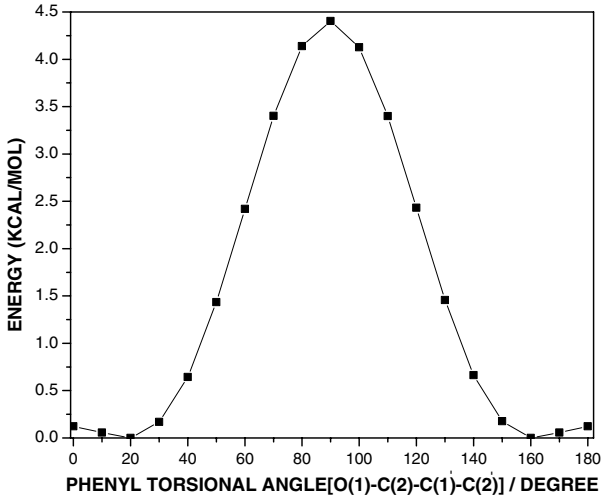

Fig. 4. Torsional potential of 5HF as phenyl group is rotated from −180° to 180° with respect to the benzo-γ-pyrone ring, using DFT-B3LYP/6-31G(d) level of theory.

virtually the same for the enol (149°) and keto (148°) form. A critical analysis of the intermediate geometries with the variation of $r_{O(3)-H(1)}$ distance shows that the hydrogen atom approaches towards the centre of the intramolecular hydrogen bonded ring system with the increase of $r_{O(3)-H(1)}$ distance, approaches an optimum distance at $r_{O(3)-H(1)} =$ 1.3 Å and then coming out of the IMHB ring with further increase of $r_{O(3)-H(1)}$ distance until it takes the appropriate orientation to form the stable keto tautomer. Therefore it becomes clear that by freezing the geometry of 5HF or by fixing the O(2)–O(3) distance at a particular values, one may ends up introducing artificial constraints on the system and hence a barrier for the enol (N) to keto (T) conversion.

In this article we used the "distinguished co-ordinate" approach as proposed by Sobolewski et al. [56] where O(3)–H(1) bond distance is varied and rest of the structural parameters are allowed to relax for each choice of $r_{O(3)-H(1)}$. Catalan et al. [48] also used the similar reaction co-ordinate (r_{O-H}) for the ESIPT processes of some naphthalene derivatives. Maheswari et al. [57] did an extensive theoretical study on salicylic acid and showed that the variation of (O–H) bond length of hydroxyl group can be used as reaction co-ordinate in order to get some idea about the PE curve for the ground as well as for the excited state proton transfer processes. In a recent communication [58], we reported that the distinguished co-ordinate approach is quite useful in understanding both the ground and excited state potential energy surface of 1-hydroxy-2-naphthaldehyde and 2-hydroxy-3-naphthaldehyde.

3.1. Barrier for phenyl rotation

Barrier to single bond internal rotation have been studied frequently by computational methods to determine relative energies for different conformations of various molecules [59,60]. Fig. 4 shows a plot of the relative energy of different rotamers of 5HF vs. the torsional angle of phenyl group with respect to the benzo-γ-pyrone plane. 5HF has lowest energy as the phenyl group is rotated by 18.7°. Crystal structure analysis of 5HF by Shoja et al. [54] showed that the phenyl group is twisted by 5.8(4)° out of plane with respect to the benzo-γ-pyrone ring. From Fig. 4, it is obvious that 5HF has low energy barrier towards the co-planar conformation and a high energy barrier towards the perpendicular conformation. DFT/B3LYP-6-31G(d) level of theory predicts that the barrier for the perpendicular and co-planar conformer of 5HF with respect to the twisted one are 4.4 and 0.1 kcal/mol, respectively. So the barrier for co-planar conformer is within the range of thermal energy (KT). Our calculation shows that the energy of the twisted conformer-I (18.7°) and conformer-II (5.8°) are very close to each other. Since, within the crystal lattice a number of molecules are closely packed, it seems due to some weak non-covalent interactions among the neighboring molecules, twisted conformer-II is the stable conformer found from X-ray crystal structure study.

3.2. Ground and excited state potential energy curve of 5HF

Fig. 5 shows the variation of potential energy along the proton transfer co-ordinate, i.e., $r_{O(3)-H(1)}$ for both the ground and the first excited singlet state of 5HF. Ground state calculation shows a minimum on the PE curve at $r_{O(3)-H(1)}$ distance near about 1.00 Å and this is due to the 'N' form of 5HF. Surprisingly, there is no shallow minima for the 'T' form, rather the ground state potential energy curve increases steadily as the $r_{O(3)-H(1)}$ distance increases from 1 to 2 Å. FC potential energy curve for the S_1 state shows two minima, one at $r_{O(3)-H(1)} = 1$ Å

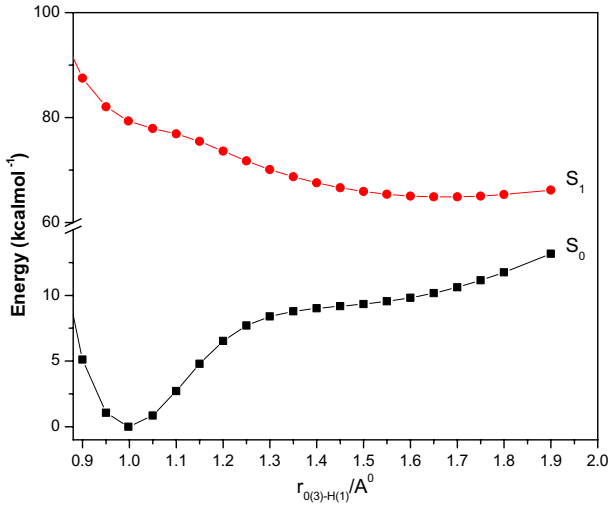

Fig. 5. GSIPT curve (S_0) and ESIPT Franck-Condon curves of 5HF as obtained from DFT-B3LYP/6-31G(d) and TD-DFT-B3LYP/6-31G(d) level of theory.

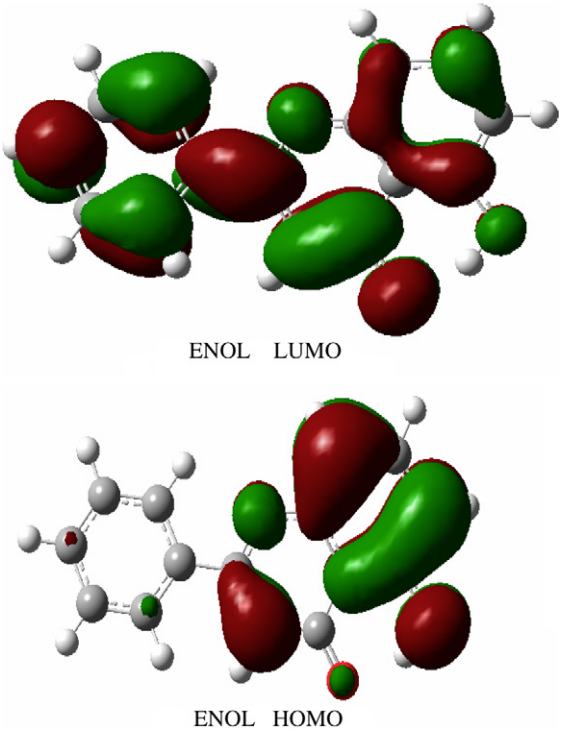

Fig. 6. HOMO and LUMO of 5HF (enol) as obtained with DFT-B3LYP/6-31G(d) level of theory.

and other which is much lower in energy is near about $r_{O(3)–H(1)} = 1.60$ Å. The former is due the excited enol form (N*) and the latter minima is due to excited keto tautomer (T*). Repulsive nature of the GSIPT curve and the energy gap between S_0 and S_1 curve at the keto tautomer position ($r_{O(3)–H(1)} = 1.60$ Å) predicts that the keto tautomer emission will be broad, structureless and red shifted. In their laser induced fluorescence measurements Chou et al. [17] showed a large stokes shifted, extremely weak broad emission band of 5HF maximized at ~700 nm for the keto tautomer resulted from ESIPT.

The repulsive nature of the ground state PE curve outright discards the possibility of the ground state intramolecular proton transfer in 5HF. Again our free energy calculations for the enol keto equilibria of 5HF give a positive value of free energy change ($\Delta G = 10.7$ kcal/mole) and the calculated equilibrium constant is $\sim 1.43 \times 10^{-10}$. On the basis of the equilibrium constant, the population ratio in the gas phase for the enol vs. keto form in the ground state is 7×10^{10}:1. This explains that GSIPT is not thermodynamically favorable. Experimental investigations of Chou et al. [17] showed that λ_{max} of 5HF in cyclohexane is nearly 350 nm. On the other hand, our calculated value of λ_{max} in the gas phase is near about 385 nm and this is in good agreement with their experimental findings.

3.3. HOMO, LUMO electron density

Analysis of the electron density of HOMO and LUMO of 5HF can through some light on the ground and excited states proton transfer processes. Both HOMO and LUMO are of π type. HOMO of enol form predicts that intramolecular hydrogen bonded (IMHB) ring system (Fig. 6) is primarily of bonding character over the O(3)H(1) and C(5)C(10) atoms, where as C(4) is anti-bonding character. Both the hydroxyl oxygen (O(3)) and carbonyl oxygen(O(2)) have bonding character, with a larger electron density over the hydroxyl oxygen(O(3)). Electron density of HOMO of keto tautomer around IMHB ring shows antibonding character over the H(1)O(3), O(3)C(5) and C(4)O(2) atoms and bonding character over the C(5)C(10)C(4) atoms. Again compare to HOMO of enol form, HOMO of keto shows much larger electron density on O(3). HOMO electron density for both the enol and keto form show less electron density over the phenyl ring.

LUMO of 5HF is π* in nature. If we look into the electronic charge distribution of LUMO (Fig. 6) within IMHB ring of N-tautomer, C(5)C(10) position have bonding character, whereas C(10)C(4), C(4)O(2) and C(3)C(5) have antibonding character. LUMO of the enol tautomer possess high electron density on O(2). After tautomerization, LUMO of keto-tautomer (Fig. 7) still shows larger electron density on O(2) and comparatively smaller density on O(3). Thus it favours the transfer of a proton from O(3) to O(2) in the excited state. Again our calculation of electron density over the proton transfer co-ordinate in the excited states (i.e., LUMO electron densities) show that there is a shift of π-electron distribution from O(3) to O(2).

Analysis of electron density of HOMO for enol tautomer (N) predicts O(2) has slightly higher bonding character than O(3). On the other hand, HOMO electron density of keto tautomer (T) of 5HF shows greater bonding character of O(3) than O(2) and hence transfer of proton from O(3) to O(2) in the ground state is quite impossible.

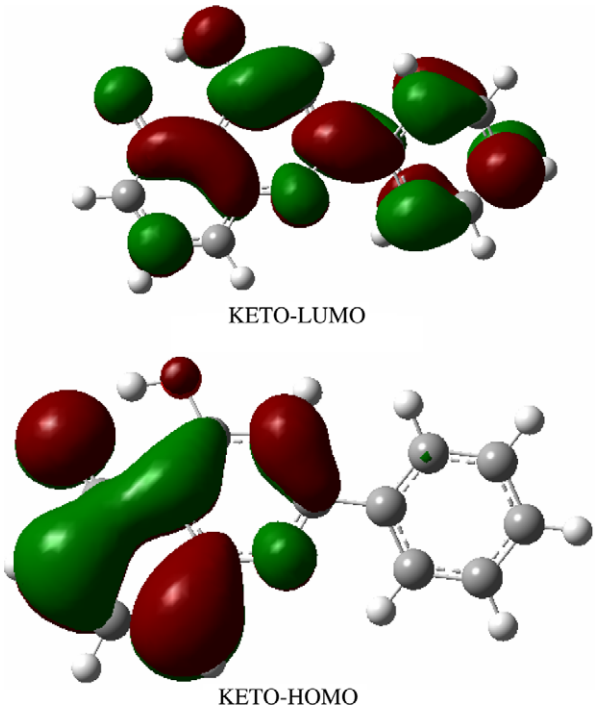

Fig. 7. HOMO and LUMO of 5HF (keto) as obtained with DFT-B3LYP/6-31G(d) level of theory.

4. Conclusions

Our PES calculations of 5HF suggest that excited keto tautomer (T^*) has much lower energy than excited enol tautomer (N^*) in their first excited singlet state. Again the energy gap between the excited singlet and ground singlet and the other low lying excited states is quite small compare to our previously studied [58] compounds, i.e., 1-hydroxy-2-naphthaldehyde and 2-hydroxy-3-naphthaldehyde. According to the energy gap law, non-radiative transition of 'T^*' to the ground state will be faster enough and there will be a competition between the radiative and non-radiative transition. We believe, due to the faster formation rate of 'T^*' (as it is obvious from the exothermic nature of the excited state potential energy surface) and also the presence of other faster non-radiative deactivation channel from 'N^*' as well as 'T^*', quantum yield of emission from both the excited enol (N^*) and keto (T^*) tautomer of 5HF would be very low. Again, the small energy gap between 'T^*' and 'T' and the repulsive nature of the ground state potential energy surface of the proton transfer form 'T' explain the red shifted broad structureless excited state proton transfer emission band of 5HF. Analysis of HOMO, LUMO π-electron density shows that the electron density on the hydroxyl oxygen (O(3)) is quite high compare to the carbonyl oxygen(O(2)) of the 'N' tautomer. Again, after the transfer of proton along the proton transfer co-ordinate shows the same oxygen atom, i.e., (O(3)) has higher electron density than O(2) in the 'T' form. This nicely explains the non-viability of ground state electron transfer. On the other hand, the LUMO electron density shows a drift of electron cloud from O(3) to O(2) along the proton transfer co-ordinate and explaining the viability of ESIPT process. Since all the calculations have been carried out by DFT method with hybrid functional, B3LYP/6-31G(d), it once again supports the potentiality of DFT method for the calculation of ESIPT process.

Acknowledgement

We gratefully acknowledge the financial support received from DST (Ref. No. SR/FTP/PS-60/2003) and UGC, New Delhi for carrying out this research work.

Appendix A. Supplementary data

Supplementary data associated with this article can be found, in the online version, at doi:10.1016/j.theochem.2007.08.014.

References

[1] N. Agmon, J. Phys. Chem. A 109 (2005) 13.
[2] S.J. Formosinho, L.G. Amaut, J. Photochem. Photobiol. A: Chem. 75 (1993) 21.
[3] G.D. Carlo, N. Mascolo, A.A. Izzo, F. Capasso, Life Sci. 65 (1999) 337.
[4] P.C.H. Hollman, I.C.W. Arts, J. Sci. Food Agric. 80 (2000) 081.
[5] S.A. Ahcrne, N.M. O'Brien, Nutrition 18 (2002) 75.
[6] F. Shahidi, P.K.J.P.D. Wanasundara, Crit. Rev. Food Sci. Nutr. 32 (1992) 67.
[7] T. Matsuura, Afinidad 343 (1977) 48.
[8] R.J. Williams, J.P.E. Spencer, C. Rice-evans, Free Radic. Biol. Med. 36 (2004) 838.
[9] M. Sarkar, P.K. Sengupta, Chem. Phys. Lett. 179 (1991) 68.
[10] V.G. Pivovarenko, A.V. Tuganova, A.S. Klymchenko, A.P. Demchenko, Cell. Mol. Biol. Lett. 2 (1997) 335.
[11] A.S. Klymchenko, A.P. Demchenko, Langmuir 18 (2002) 5637.
[12] O.P. Bondar, V.G. Pivovarenko, E.S. Rowe, Biochim. Biophys. Acta 1369 (1998) 119.
[13] A. Klymchenko, G. Duportail, T. Ozturk, V. Pivovarenko, Y. Mily, A. Demchenko, Chem. Biol. 9 (2002) 1199.
[14] V.V. Shynkar, A.S. Klymchenko, Y. Mely, G. Duportail, V.G. Pivovarenko, J. Phys. Chem. B. 108 (2004) 18750.
[15] A.D. Roshal, A.V. Grigorovich, A.D. Doroshenko, V.G. Pivovarenko, A.P. Demchenko, J. Photochem. Photobiol A: Chem. 127 (1999) 89.
[16] X. Poteau, G. Saroja, C. Spies, R.G. Brown, J. Photochem. Photobiol. A Chem. 162 (2004) 431.
[17] P.-T. Chou, Y.-C. Chen, W.-S. Yu, Y.-M. Cheng, Chem. Phys. Lett. 340 (2001) 89.
[18] A. Weller, Z. Elektrochem. 60 (1956) 1144.
[19] F. Lahmani, A. Zehnacker-Rentien, J. Phys. Chem. A 101 (1997) 6141.
[20] D. Gormin, A. Sytnik, M. Kasha, J. Phys. Chem. A 101 (1997) 672.
[21] P.F. McGarry, S. Jockusch, Y. Fujiwara, N.A. Kaprinidis, N.J. Turro, J. Phys. Chem. A 101 (1997) 764.
[22] V. Guallar, M. Moreno, J.M. Lluch, F. Amat-Guerri, A. Douhal, J. Phys. Chem. 100 (1996) 19789.
[23] J. Keck, H.E.A. Kramer, H. Port, T. Hirsch, P. Fischer, G. Rytz, J. Phys. Chem. 100 (1996) 14468.
[24] F. Parsapour, D.F. Kelley, J. Phys. Chem. 100 (1996) 2791.
[25] R.M. Tarkka, S.A. Jenekhe, Chem. Phys. Lett. 260 (1996) 533.
[26] H. Zhang, P. van der Meulen, M. Glasbeek, Chem. Phys. Lett. 253 (1996) 97.

[27] S. Mitra, R. Das, S.P. Bhattacharyya, S. Mukherjee, J. Phys. Chem. A 101 (1997) 293.
[28] P.G. Yi, Y.H. Liang, C.Z. Cao, Chem. Phys. 315 (2005) 297.
[29] S. Nagaoka, U. Nagashima, J. Phys. Chem. 94 (1990) 1425.
[30] S. Nagaoka, U. Nagashima, Chem. Phys. 136 (1989) 153.
[31] M.V. Verner, S. Scheiner, J. Phys. Chem. 99 (1995) 642.
[32] A.L. Sobolewski, W. Domcke, Chem. Phys. 184 (1994) 115.
[33] J. Catalan, J. Palomar, J.L.G. De Paz, J. Phys. Chem. A 101 (1997) 7914.
[34] K.-Y. Law, J. Shoham, J. Phys. Chem. 98 (1994) 3114.
[35] K.-Y. Law, J. Shoham, J. Phys. Chem. 99 (1995) 12103.
[36] A.U. Acuna, F. Toribio, F. Amat-Guerri, J. Catalan, J. Photochem. 30 (1985) 339.
[37] F. Toribio, J. Catalan, F. Amat, A.U. Acuna, J. Phys. Chem. 87 (1983) 817.
[38] A.U. Acuna, F. Amat-Guerri, J. Catalan, F. Gonzalez-Tablas, J. Phys. Chem. 84 (1980) 629.
[39] J. Goodman, L.E. Brus, J. Am. Chem. Soc. 100 (1978) 7472.
[40] K.K. Smith, K.J. Kaufmann, J. Phys. Chem. 82 (1978) 2286.
[41] S. Nagaoka, N. Hirota, M. Sumitani, K. Yoshihara, J. Am. Chem. Soc. 105 (1983) 4220.
[42] T. Nishiya, S. Yamauchi, N. Hirota, M. Baba, I. Hanazaki, J. Phys. Chem. 90 (1986) 5730.
[43] L.A. Peteanu, R.A. Mathies, J. Phys. Chem. 96 (1992) 6910.
[44] M.A. Morgan, E. Orton, G.C. Pimentel, J. Phys. Chem. 94 (1990) 7927.
[45] S. Nagaoka, N. Hirota, M. Sumitani, K. Yoshihara, E. Lipezynska-Kochany, H. Iwamura, J. Am. Chem. Soc. 106 (1984) 6913.
[46] S. Nagaoka, U. Nagashima, N. Ohta, M. Fujita, T. Takemura, J. Phys. Chem. 92 (1988) 166.
[47] J. Catalan, F. Toribio, A.U. Acuna, J. Phys. Chem. 86 (1982) 303.
[48] J. Catalan, J.C. del Valle, J. Palomer, C. Diaz, J.L.G. dePaz, J. Phys. Chem. A 103 (1999) 10921.
[49] A. Bouchy, D. Rinaldi, J.-L. Rivail, Int. J. Quant. Chem. 96 (2004) 273.
[50] A. Dreuw, M. Head-Gordon, Chem. Rev. 105 (2005) 4009.
[51] A.D. Becke, J. Chem. Phys. 98 (1993) 5648;
C. Lee, W. Yang, R.G. Parr, Phys. Rev. B 37 (1988) 785.
[52] V. Barone, C. Adamo, J. Phys. Chem. 99 (1995) 15062.
[53] Gaussian 03, Revision C.02, M.J. Frisch, G.W. Trucks, H.B. Schlegel, G.E. Scuseria, M.A. Robb, J.R. Cheeseman, J.A. Montgomery, Jr., T. Vreven, K.N. Kudin, J.C. Burant, J.M. Millam, S.S. Iyengar, J. Tomasi, V. Barone, B. Mennucci, M. Cossi, G. Scalmani, N. Rega, G.A. Petersson, H. Nakatsuji, M. Hada, M. Ehara, K. Toyota, R. Fukuda, J. Hasegawa, M. Ishida, T. Nakajima, Y. Honda, O. Kitao, H. Nakai, M. Klene, X. Li, J.E. Knox, H.P. Hratchian, J.B. Cross, C. Adamo, J. Jaramillo, R. Gomperts, R.E. Stratmann, O. Yazyev, A.J. Austin, R. Cammi, C. Pomelli, J.W. Ochterski, P.Y. Ayala, K. Morokuma, G.A. Voth, P. Salvador, J.J. Dannenberg, V.G. Zakrzewski, S. Dapprich, A.D. Daniels, M.C. Strain, O. Farkas, D.K. Malick, A.D. Rabuck, K. Raghavachari, J.B. Foresman, J.V. Ortiz, Q. Cui, A.G. Baboul, S. Clifford, J. Cioslowski, B.B. Stefanov, G. Liu, A. Liashenko, P. Piskorz, I. Komaromi, R.L. Martin, D.J. Fox, T. Keith, M.A. Al-Laham, C.Y. Peng, A. Nanayakkara, M. Challacombe, P.M.W. Gill, B. Johnson, W. Chen, M.W. Wong, C. Gonzalez, and J.A. Pople, Gaussian, Inc., Wallingford, CT, 2004.
[54] M. Shoja, Acta cryst. C 46 (1990) 517.
[55] M.V. Vener, S. Scheiner, J. Phys. Chem. 99 (1995) 642.
[56] A.L. Sobolewski, W. Domcke, Chem. Phys. 232 (1998) 257.
[57] S. Maheshwari, A. Chowdhury, N. Sathyamurthy, H. Mishra, H.B. Tripathi, M. Panda, J. Chandrasekhar, J. Phys. Chem. A 103 (1999) 6257.
[58] S.P. De, S. Ash, S. Dalai, A. Misra, J. Mol. Struct. (THEOCHEM). 807 (2007) 33.
[59] J.P. Conard, J.C. Merlin, A.C. Boudet, L. Vrielynk, Biospectroscopy 3 (1997) 183.
[60] A. Karpfen, C.H. Choi, M. Kertesz, J. Phys. Chem. A 101 (1997) 7426.